OPTOELECTRONICS AND ADVANCED MATERIALS – RAPID COMMUNICATIONS Vol. 12, No. 9-10, September-October 2018, p. 617 - 621

Preparation of PS@TiO_2 composited particles and their visible light photocatalytic properties

XIAOLIANG ZHANG[a,b,*], CHUNXIA WU[a,*], YI REN[a], WENSHU YANG[a], HONGWEI CHE[b], JINGBO MU[b]
[a]*College of Material Science and Engineering, Hebei University of Engineering, Handan 056038, P. R. China*
[b]*Institute of Novel Materials for Energy and Environment, Hebei University of Engineering, Handan 056038, P. R. China*

PS@TiO_2 core-shell composited particles (CSCPs) were prepared by self-assembly technique. Photocatalytic activity of PS@TiO_2 CSCPs for the degradation of Rhodamine B (RB) is much better than that of pure PS or TiO_2 particles. Results suggest that PS@TiO_2 CSCPs with four layers of TiO_2 colloids shell show the optimum photocatalytic activity. When the solution concentration of HCl is 0.6 M and the size of PS particle cores are 2 µm, the as-prepared PS@TiO_2 CSCPs have the optimum synergistic photocatalytic activity. The PS@TiO_2 CSCPs materials obtained by this method can be used to degrade the RB dye efficiently.

(Received February 11, 2018; accepted October 10, 2018)

Keywords: Titanium dioxide (TiO_2), Polystyrene (PS), Composited Particles, Rhodamine B (RB), Photocatalytic properties

1. Introduction

In recent several decades, environmental pollution has become a solemn problem which affects people’s lives and healthy [1-4]. Titanium dioxide (TiO_2) has strong oxidation ability, low cost, good stability and no light corrosion, which is considered to be the leading catalyst for environmental purification [5-9]. However, TiO_2 is only vigorous in the ultraviolet (UV) light [10]. A great quantity of research scholars have focused their attentions on modification of TiO_2 by doping or compounding with other materials, and improved their photocatalytic properties under visible-light irradiation [11-16]. Because of their composited composition, excellent arrangement, and the properties of multiple particles, polymer/inorganic composites are attracting a lot of attention [17].

Owing to easy preparations, controllable sizes, excellent adsorption ability, and large surface areas, polystyrene (PS) spheres are very suitable as the cores or templates for preparations of polymer/inorganic composites [18-25]. Deng group fabricated PS/Ag nanocomposite spheres through utilizing the dual functions of PVP, and found that the PS/Ag nanocomposite spheres exhibit excellent catalytic properties for the reduction of organic dyes [26]. Moreover, their research indicates that these PS/Ag nanocomposite spheres possess extraordinary antibacterial abilities against Salmonella and Escherichia coli. Wang and co-workers prepared core/shell PS@TiO_2 photocatalyst in the absence of surfactant by a vapor phase hydrolysis process [27]. They found that the core/shell catalyst has a relatively higher activity in the degradation of methylene blue (MB) than that of bare TiO_2 due to the improved floating and light harvesting ability [27]. Wang and co-workers synthesized PS@CdS core-shell structure nanoparticles with 260 nm core and a uniform shell by sonochemical method [20]. The shell thickness could be adjusted by changing the reaction time and the molar ration. Compared to the pure CdS, the PS@CdS core-shell structure nanoparticles exhibited good photocatalytic activity for the degradation of RB, which benefits from the synergic effect between the core and the shell [20]. Türk and colleagues prepared PS colloidal particles with TiO_2 coating via an emulsifier-free emulsion copolymerization and a sol-gel process in-situ hydrolysis and a condensation reaction [28]. They found that the PS/TiO_2 core/shell particles revealed good photocatalytic activity for the oxidation of 4-methoxybenzyl alcohol with O_2 in water [28]. Wu group prepared PS/TiO_2 nanocomposite particles by using aqua ammonia/triethanolamine as the positive/negative catalyst pair. They found that when the reaction temperature was increased during TiO_2 coating process, the surface morphology of the TiO_2 shell became defective and the roughness on the surface of the TiO_2 shell was remarkably heightened [29].

In this study, PS@TiO_2 core-shell composited particles (CSCPs) were prepared by layer-by-layer self-assembly method. The influences of the solution concentration of HCl, the number of TiO_2 colloids shell layers and the size of PS particle core on structure of CSCPs and the degradation rate of RB were carefully studied. Scanning electron microscopy (SEM), UV-visible spectrophotometer, and other analytical methods were adopted for the study of the synthesized materials. The PS@TiO_2 CSCPs system has the characteristics of stable and does not produce secondary pollution. It has been a great concern in the field of environmental pollution and shows a broad application prospects.

2. Experimental methods

Monodisperse polystyrene (PS) microspheres were purchased from Tianjin BaseLine ChromTech Research Centre. Ammonium hydroxide (NH_3 28%), sodium dodecyl sulphate (SDS), hydrochloric acid (HCl) and anhydrous alcohol were purchased from Yantai double Chemical Co., Ltd. and used as received. Titanium tetrachloride ($TiCl_4$), Rhodamine B (RB), acetone and anhydrous sodium sulphate (Na_2SO_4) were purchased from Tianjin Oubokai Chemical Co. Ltd. and used as received.

Monodisperse PS particles were centrifuged firstly, followed centrifugal cleaned sequentially with deionized water, NH_3, HCl, anhydrous alcohol and deionized water for 20 min, respectively. The SDS self assembled monolayer (SAM) were prepared by immersing the PS particles into the solution of SDS (5 mmol/L) for 2 h, subsequently rinsed with deionized water and dried in an oven. The PS particles with SDS SAM were immersed in a TiO_2 colloidal solution at 80 ℃ for 2 h. The TiO_2 colloidal solution was prepared in advance by using $TiCl_4$ and HCl according to the literatures [30-31]. The PS@TiO_2 composited particles were placed at room temperature (25 ℃) for 24 h. Afterwards, the PS@TiO_2 CSCPs with one layer of TiO_2 colloids shell were successively centrifuged, ultrasonic cleaned with deionized water and dried. The PS@TiO_2 CSCPs with multi-layers of TiO_2 colloids shell were prepared by repeating the above procedures. The surface morphology of PS@TiO_2 CSCPs was characterized by Hitachi SU8200 FESEM. The constituents of the PS@TiO_2 CSCPs were characterized by using energy dispersive x-ray analysis (EDAX).

The light photocatalytic performances of PS@TiO_2 CSCPs with multi-layers of TiO_2 colloids shell were evaluated by the degradation of Rhodamine B (RB) in an aqueous solution containing 80 mL RB dye (10 mg/L) and 0.1 mg/mL PS@TiO_2 CSCPs. The RB solution with PS@TiO_2 CSCPs was stirred vigorously while it was irradiated by simulate sunlight (HSX-UV300, high pressure 160 W xenon lamp light). A T-6 UV-visible spectrophotometer was used to determine and analyze the extent of photodegradation at the wavelength of 553 nm.

3. Results and discussion

3.1. Characterization of PS@TiO_2 CSCPs

Fig. 1 shows the FESEM images of PS particles and PS@TiO_2 CSCPs. It can be seen from Fig. 1(a) that the diameter of PS particles is approximately 2 μm. The shapes of PS particles are neatly spherical, and the surface of PS particles is clean and smooth. As shown in Fig. 1(b), the surface of PS@TiO_2 CSCPs is a little irregular and rough. Fig. 1(c) is the EDAX of the red selected area on the Fig. 1(b). It can be seen that TiO_2 colloids were assembled on the surface of PS particles.

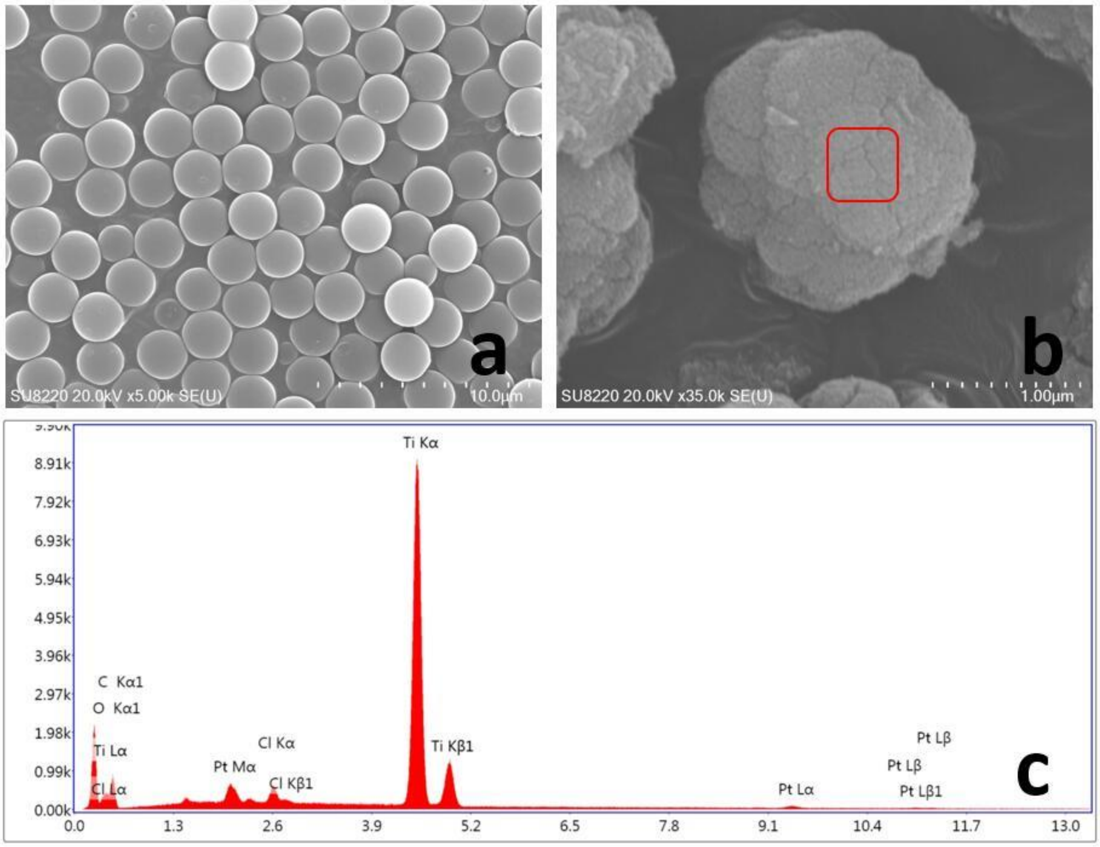

Fig. 1. FESEM images of PS particles and PS@TiO_2 CSCPs. (a) 2 μm PS particles, (b) 2 μm PS@TiO_2 CSCPs, (c)EDAX of the red selected area in (b)

Fig. 2 shows the FESEM image of the PS@TiO$_2$ CSCPs with four layers of TiO$_2$ colloids shell at different solution concentration of HCl. There are some agglomerations for the PS@TiO$_2$ CSCPs. It can be seen that the surface features of PS@TiO$_2$ CSCPs at different solution concentration of HCl are slightly different. However, the agglomeration did not weaken the photocatalytic activity of PS@TiO$_2$ CSCPs for degradation of RB, and the photocatalytic activities is different when the solution concentration of HCl is changed. The small TiO$_2$ colloids clusters on surfaces of PS particles increased with increasing HCl concentration. The surface of PS@TiO$_2$ CSCPs for 0.6 M HCl is uniform and relatively clean.

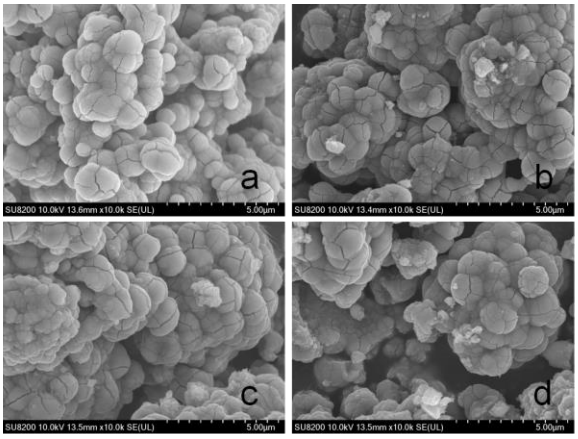

Fig. 2. FESEM images of 2 μm PS@TiO$_2$ CSCPs at different solution concentration of HCl. (a) 0.1 M HCl, (b) 0.3 M HCl, (c) 0.6 M HCl, (d) 1.0 M HCl

3.2. Photocatalytic activity

Fig. 3 shows the degradation rate of RB with reaction time for 2 μm PS particles with different layers of TiO$_2$ colloids shell. It can be seen that the degradation rate of RB is very slow under irradiation conditions without any photocatalyst (the blank sample), and only approximately 6% RB was degraded at 30 min. Photocatalytic activity of PS@TiO$_2$ CSCPs is better than that of single PS or TiO$_2$ particles. For the pure PS sample, the degradation rate of RB was approximately 15% at 30 min. The degradation rate of RB was approximately 36% at 30 min for the pure TiO$_2$ sample. When the PS particles were composited with TiO$_2$ colloids shell, the degradation rate of RB accelerated rapidly, which is due to the synergistic photocatalytic activity between the PS particle core and TiO$_2$ colloids shell. Moreover, the degradation rate of RB increased with increasing number of TiO$_2$ colloids shell layers. When the number of TiO$_2$ colloids shell layer increased to four or more, the degradation rates of RB were very similar, and all degradation rates of RB were approximately 93% at 30 min. When the number of TiO$_2$ colloids shell layers increased, the synergistic photocatalytic activity between the PS particle core and TiO$_2$ colloids shell is better. As the number of TiO$_2$ colloids shell layer increased to four or more, the synergistic photocatalytic activities are similar. From the point of view of saving materials, PS@TiO$_2$ CSCPs with four layers of TiO$_2$ colloids shell are the optimum photocatalyst.

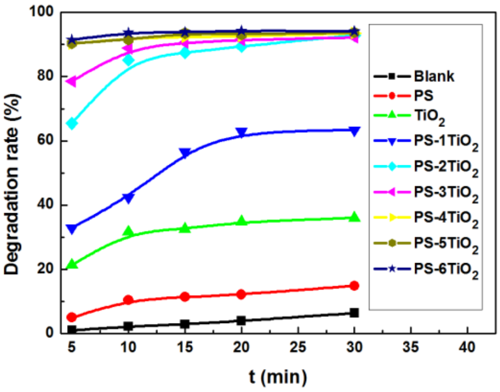

Fig. 3. Degradation rate of RB with reaction time for 2 μm PS@TiO$_2$ CSCPs with different layers of TiO$_2$ colloids shell

Fig. 4 shows the degradation rate of RB with reaction time for as-prepared 2 μm PS@TiO$_2$ CSCPs under different solution concentration of HCl conditions. It can be seen that the degradation rate of RB for as-prepared PS@TiO$_2$ CSCPs under 0.3 M HCl condition is slightly higher than that under 0.1 M HCl condition. The degradation rate of RB quickly reaches approximately 60% at 5 min, and reaches approximated 80% at 30 min for as-prepared PS@TiO$_2$ CSCPs under 0.1 M HCl condition. When the solution concentration of HCl is 0.6 M, the degradation rate of RB of the as-prepared PS@TiO$_2$ CSCPs is 90% and 93% at reaction time of 5 min and 30 min. The degradation rate of RB of the as-prepared PS@TiO$_2$ CSCPs under 1.0 M HCl condition is lower than that under other concentrations of HCl conditions. When the solution concentration of HCl is 0.6 M, the size of TiO$_2$ colloids clusters on surfaces of PS is more relatively uniform, resulting in the best synergistic photocatalytic activity between the PS particle core and TiO$_2$ colloids shell.

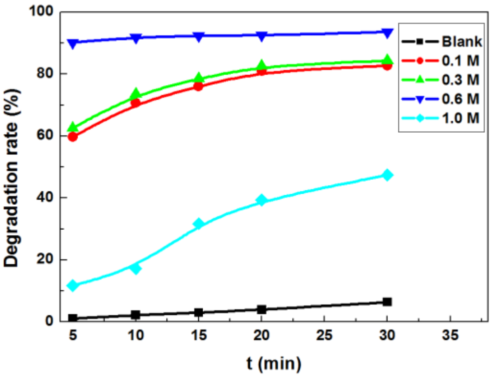

Fig. 4. Degradation rate of RB with reaction time for as-prepared 2 μm PS@TiO$_2$ CSCPs under different solution concentration of HCl conditions

Fig. 5 shows the degradation rate of RB for PS@TiO_2 CSCPs with different size of PS particle core. For 0.5 μm PS@TiO_2 CSCPs, the degradation rate of RB is approximately 16% at 5 min, and the degradation rate of RB can be reached 39% at 30 min. For the 2 μm PS@TiO_2 CSCPs, the degradation rate of RB is approximately 90% at 5 min, and the degradation rate of RB can be reached 93% at 30 min. For the 10 μm PS@TiO_2 CSCPs, the degradation rate of RB is approximately 31% at 5 min, and the degradation rate of RB can be reached 59% at 30 min. For the 25 μm PS@TiO_2 CSCPs, the degradation rate of RB is approximately 32% at 5 min, and the degradation rate of RB can be reached 45% at 30 min. Because the size of TiO_2 colloids clusters is approximately 1.3 μm, the synergistic photocatalytic activity is low for the 0.5 μm cores. When the size of cores (10 μm or 25 μm) is much larger than that of TiO_2 colloids clusters, the synergistic photocatalytic activity is still weak. Only when the size of the cores is close to or slightly larger than that of the TiO_2 colloids clusters, the as-prepared PS@TiO_2 CSCPs have the best synergistic photocatalytic activity between the PS particle core and TiO_2 colloids shell, and the photocatalytic result is even more dramatic.

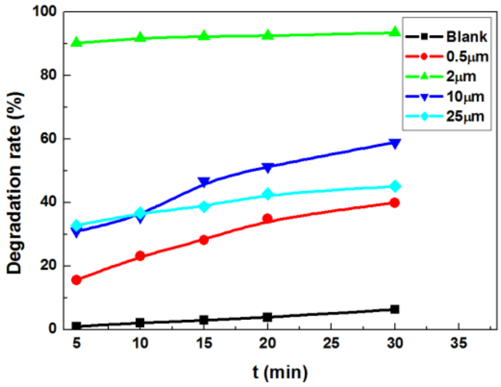

Fig. 5. Degradation rate of RB for PS@TiO_2 CSCPs with different size of PS particle core

4. Conclusion

PS@TiO_2 CSCPs have been prepared by layer-by-layer self assembly technique. The experimental results showed that the photocatalytic activity of PS@TiO_2 CSCPs for the degradation of RB is better than that of pure PS or TiO_2 particles. The degradation rate of RB increased with increasing number of TiO_2 colloids shell layer. When the number of TiO_2 colloids shell layer reaches four, the degradation rate of RB is approximately 90% at 5 min, and the degradation rate of RB can be reached 93% at 30 min. When the size of PS particle cores are 2 μm and the solution concentration of HCl is 0.6 M, the as-prepared PS@TiO_2 CSCPs have the best synergistic photocatalytic activity between the PS particle core and TiO_2 colloids shell, and the photocatalytic result is most satisfying. The PS@TiO_2 CSCPs materials obtained by this method will be possibly potential applications for water purification photocatalysis.

Acknowledgements

This work is financially supported by National Natural Science Foundation of China (Grant No. 51405131), Young Talents of Colleges and Universities of Hebei Province (Grant No. BJ2016009) and Natural Science Foundation of Hebei Province (Grant Nos. E2015402088).

References

[1] S. Jeong, H. Cho, S. Han, P. Won, H. Lee, S. Hong, J. Yeo, J. Kwon, S. H. Ko, Nano Lett. **17**(7), 4339 (2017).
[2] J. Shang, M. Chai, Y. F. Zhu, Environ. Sci. Technol. **37**(19), 4494 (2003).
[3] X. U. Zhao, Z. W. Li, Y. Chen, L. Y. Shi, Y. F. Zhu, J Mol. Catal. A-Chem. **268**(1-2), 101 (2007).
[4] W. S. Wang, J. Feng, Y. F. Ye, F. L. Lyu, Y. S. Liu, J. H. Guo, Y. D. Yin, Nano Lett. **17**(2), 755 (2017).
[5] Y. Zhang, J. R. Chen, L. Hua, S. J. Li, X. X. Zhang, W. C. Sheng, S. S. Cao, J. Hazard, Mater. **340**, 309 (2017).
[6] M. V. Sheridan, D. J. Hill, B. D. Sherman, D. G Wang, S. L. Marquard, K. R. Wee, J. F. Cahoon, T. J. Meyer, Nano Lett. **17**(4), 2440 (2017).
[7] J. A. Shi, C. L. Sun, M. B. Starr, X. D. Wang, Nano Lett. **11**(2), 624 (2011).
[8] S. Hoang, S. W. Guo, N. T. Hahn, A. J. Bard, C. B. Mullins, Nano Lett. **12**(1), 26 (2012).
[9] V. Singh, I. J. C. Beltran, J. C. Ribot, P. Nagpal, Nano Lett. **14**(2), 597 (2014).
[10] L. Song, R. L. Qiu, Y. Q. Mo, D. D. Zhang, H. Wei, Y. Xiong, Catal. Commun. **8**(3), 429 (2007).
[11] T. Eren, A. N. Okte, J. Appl. Polym. Sci. **105**(3), 1426 (2007).
[12] R. Klaysri, S. Wichaidit, S. Piticharoenphun, O. Mekasuwandumrong, P. Praserthdam, Mater. Res. Bull. **83**, 640 (2016).
[13] M. M. Kamrannejad, A. Hasanzadeh, N. Nosoudi, L. Mai, A. A. Babaluo, Mat. Res. **17**(4), 1039 (2014).
[14] D. W. Ding, K. Liu, S. N. He, C. B. Gao, Y. D. Yin, Nano Lett. **14**(11), 6731 (2014).
[15] K. K. Sakimoto, S. J. Zhang, P. D. Yang, Nano Lett. **16**(9), 5883 (2016).
[16] L. X. Kang, Y. Hu, L. L. Liu, J. X. Wu, S. C. Zhang, Q. C. Zhao, F. Ding, Q. W. Li, J. Zhang, Nano Lett. **15**(8), 403 (2015).
[17] R. G Chaudhuri, S. Paria, Chem. Rev. **112**(4), 2373 (2012).
[18] X. H. Zhao, P. Wang, N. F. Ren, Nano **9**,145007901 (2014).
[19] W. L. Shi, Y. Sahoo, M. T. Swihart, P. N. Prasad, Langmuir **21**(4), 1610 (2005).
[20] H. Wang, Q. Xu, X. Zheng, W. Q. Han, J. T. Zheng, B. Jiang, Q. Z. Xue, M. B. Wu, J. Nanopart. Res. **16**, 2794 (2014).
[21] J. H. Lee, Y. Lee, J. D. Nam, Surf. Interface Anal. **42**(1), 36 (2010).

[22] W. L. Zhang, Y. D. Liu, H. J. Choi, J. Mater. Chem. **21**(19), 6916 (2011).
[23] L. B. Sun, X. Sun, Y. H. Zheng, Q. Q. Lin, H. J. Su, Y. X. Wang, C. X. Qi, J. Appl. Polym. Sci. **134**(19), 1 (2017).
[24] G H. Sun, L. Zhang, H. C. Yin, J. T. Zheng, C. S. Zhu, B. Jiang, H. Wang, S. Qiu, J. J. Yuan, M. B. Wu, Inorg. Nano-Metal Chem. **47**(5), 737 (2017).
[25] J. M. Du, H. M. Wang, H. J. Chen, M. H. Yang, X. L. Lu, H. Guo, Z. M. Zhang, T. W. Shang, S. J. Xu, W. Q. Li, P. P. Wang, I. Shakir, Nano **11**, 1650068 (2016).
[26] Z. W. Deng, H. B. Zhu, B. Peng, H. Chen, Y. F. Sun, X. D. Gang, P. J. Jin, J. L. Wang, ACS Appl. Mater. Inter. **4**(10), 5625 (2012).
[27] F. Z. Shi, Y. G Li, H. Z. Wang, Q. H. Zhang, Appl. Catal. B-Environ. **123-124**(240), 127 (2012).
[28] R. B. Karabacak, M. Erdem, S. Yurdakal, Y. Cimen, H. Turk, Mater. Chem. Phys. **144**(3), 498 (2014).
[29] J. J. Yan, Q. Q. Yu, S. S. Wu, J. Shen, J. Thermoplast. Compos. Mater. **27**(4), 429 (2014).
[30] R. F. Chen, L. Zhang, Y. Wei, D. L. Hou, J. Mater. Sci. **42**(17), 7141 (2007).
[31] S. Yin, H. Hasegawa, D. Maeda, M. Ishitsuka, T. Sato, J. Photoch. Photobio. A **163**(1-2), 1 (2004).

---

*Corresponding author: zhangxiaoliang@hebeu.edu.cn,
chunxiawu@hebeu.edu.cn